Stress Development in Drying Coatings

H. LEI,* J. A. PAYNE,* A. V. MCCORMICK, L. F. FRANCIS, W. W. GERBERICH, L. E. SCRIVEN

Coating Process and Fundamentals Program, Department of Chemical Engineering and Materials Science and Center for Interfacial Engineering, University of Minnesota, Minneapolis, Minnesota 55455

Received 3 May 2000; accepted 1 November 2000

ABSTRACT: As a solvent-cast polymeric coating dries, each part reaches a concentration at which it solidifies and develops elastic modulus. Thereafter, as further solvent departs, that part shrinks out-of-plane, but not in-plane, if the coating adheres to its substrate. Hence, it develops in-plane elastic stress. If the stress grows large enough, the stress-free state may yield, which reduces the final stress level. A theoretical model of diffusion and mass transfer, large shrinkage-induced deformation, and elastic stress, together with yielding and postyielding viscous deformation, was developed to predict stress evolution in one-dimensional drying of polymer coatings. Concentration varies only perpendicularly to the substrate, the coating shrinks only in that direction, and the stress varies only in that direction but is in-plane isotropic. The predictions are compared with measurements of evolving stress in various solvent-cast polymer coatings and aqueous gelatin coatings by a cantilever-deflection method. © 2001 John Wiley & Sons, Inc. J Appl Polym Sci 81: 1000–1013, 2001

Key words: coating; stress; drying; elasto-viscoplastic; relaxation

INTRODUCTION

Coatings deposited as liquid are commonly solidified by chilling, drying (solvent removal), curing (chemical reaction), or a combination of these processes. This investigation addresses (1) solidification of polymer–solvent coatings deposited on solid flat substrates; (2) the stress that develops as such coatings dry; and (3) the consequences of viscoplastic yielding, if the stress exceeds the coating's yield strength at its current solvent content.

Immediately after a solution coating is deposited it is a liquid. To make up for the shrinkage that accompanies solvent loss, the remaining material moves toward the substrate as solvent evaporates. Once enough solvent evaporates so that the remaining material solidifies, it is by definition capable of supporting elastic stress. As additional solvent departs the solid by further drying, the coating is unable to shrink freely because, to be a coating, it must adhere to the substrate. This frustration of volume shrinkage causes strain, which is locally the difference between the adhering state and the equilibrium state, which is stress free (apart from isotropic ambient pressure). This strain is accompanied by stress, which is related to the modulus of the remaining material. Throughout most of a coating, the stress is solely in-plane tensile stress (at edges and inclusions more complex concentrations of stress arise). In the final coated products, stresses are the principal causes of defects such as curl, delamination, and cracking.[1,2]

The mechanisms of stress development are still under active study. Croll[3] developed a simple one-dimensional theory to estimate the in-plane

**Current address:* Eastman Kodak Company, Kodak Park, Rochester, NY 14652.

Correspondence to: H. Lei (herong.lei@kodak.com).

Contract grant sponsors: Center for Interfacial Engineering, University of Minnesota; DuPont Company.

Journal of Applied Polymer Science, Vol. 81, 1000–1013 (2001)

stress in solvent-cast thermoplastic coatings coated on rigid substrates. He assumed that drying was slow enough that the concentration does not vary with depth inside the coating. He took the stress to be solely in-plane, uniform, and proportional to the decrease in volume fraction of solvent after it passes the level at which the coating solidifies, and thereby acquires an elastic modulus. Croll's predictions of final stress level match fairly well with some measurements of final stress he made by the cantilever-deflection method. Perera and Eynde[4,5] also used the cantilever-deflection method to measure stress evolution in different coatings. Despite this progress, experimental measurements and relevant determinations of physical properties are still scarce. In a series of studies Hasatani[6,7] and Itaya et al.[8] used a finite-element method to solve equations of linear elasticity to predict shrinkage and stress development in drying clays. They considered only cases of small deformation, for which mass transport was not coupled with mechanical equilibrium. Recently, Tam et al.[9,10] were the first to model drying coatings to account for large deformation. They employed a finite-element method to solve the coupled equations of mass transfer from coating to flowing air, diffusion with convection in solvent–polymer layers, and a linear relation of stress to a quadratic measure of strain. Their constitutive relation was appropriate to compressible elastic solids, which most glassy polymers are. They examined the effects not only of the concentration gradients (neglected by Croll[3]) but also of external edges, thickness variations, and inclusions in coatings. They incorporated yield stress and postyield viscous deformation, and they explored the effect of plastic yielding. Most recently, Christodoulou and coworkers[11] also considered the large deformation in the drying gel, in which non-Fickian diffusion is coupled with the stress contributions from a hypoelastic polymer network as well as an ideal liquid solvent, although their analysis is limited to model elastic coatings.

In this study we report measurements of evolving stress in several solvent-cast polymer coatings by a cantilever-deflection method. The conditions were such that drying was one-dimensional except for edge effects, which were minor. One-dimensional in this context means that concentration varies only perpendicularly to the plane of the substrate, the coating shrinks only in that direction, and the stress varies only in that direction but is in-plane isotropic. We report theoretical analyses that, like those of Tam et al.,[9,10] account for large elastic strain and stress, as well as viscoplastic straining (nonlinear theory). The constitutive relation we use is appropriate for incompressible elastomeric solids, which most rubbery polymers are. The analysis is specialized for one-dimensional drying, an instructive generalization of Croll's elementary model. In this case the governing equations reduce to relatively simple form: a partial differential equation of diffusion in one dimension, a first-order ordinary differential equation of evolution of the stress-free state at each location, and algebraic equations of boundary conditions and constraint (Amagat's condition of additivity of partial volumes, incompressibility). Solving this system and interpreting the solution are comparatively straightforward. We compare solutions with the results of stress measurement.

THEORY

Diffusion of Solvent in Coating and Mass Transfer in Gas

Drying couples not only mechanics and mass transport, but also heat transfer. For solvent to evaporate from the free surface of a coating, its latent heat of vaporization must be supplied there. Conduction through the substrate, convection by the flowing gas, and radiation from surroundings may contribute. These may not be rapid enough to avoid evaporative cooling of a solvent coating when it is first deposited. However, by the time the coating surface has solidified, evaporation has slowed and heat transfer to and within the layer is so much more rapid than mass transfer that the coating's temperature is uniform; hence, heat transfer is not considered here.

Provided the externally imposed air flow, temperature, and solvent partial pressure are uniform, a deposited coating can dry and solidify uniformly in-plane (Fig. 1). In this one-dimensional regime the conservation equations of solvent S and polymer P in the coating are[12]

$$\frac{\partial c_S}{\partial t} + \frac{\partial n_S}{\partial z} = 0, \quad \frac{\partial c_P}{\partial t} + \frac{\partial n_P}{\partial z} = 0 \tag{1}$$

where the n_i are the molar fluxes and c_i are the molar concentrations. In a drying coating, the solvent and polymer move at different average

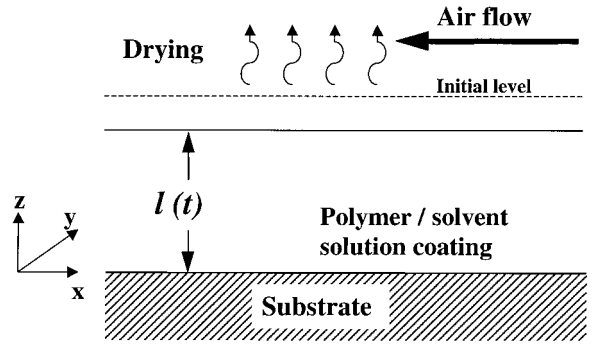

Figure 1 One-dimensional drying. Concentration and stress vary only in the z-direction. Material moves only in that direction. Stress is biaxial tension in the xy-planes. The coating thickness $l(t)$ decreases as drying proceeds.

velocities, v_S and v_P, with respect to a substrate-fixed frame. The local volume-average velocity v^a with respect to the fixed frame is then

$$v^a = c_S\bar{V}_S v_S + c_P\bar{V}_P v_P \tag{2}$$

where $\bar{V}_i$ are partial molar volumes. The $\bar{V}_i$ in general depend on composition, but when solvent and polymer mix ideally, $\bar{V}_S$ and $\bar{V}_P$ are constants. Even when mixing is mildly nonideal, constants are often a good approximation. In either case, the concentrations of solvent and polymer are related by Amagat's law:

$$c_S\bar{V}_S + c_P\bar{V}_P = 1 \tag{3}$$

This relation couples the two component conservation equations. Only one of the equations in (1) needs to be solved.

At the impermeable substrate, the fluxes of solvent and polymer are zero. From eqs. (1)–(3) it follows that the volume average velocity vanishes throughout the coating. In that case the molar fluxes are the same as the diffusive fluxes, relative to the volume average velocity. The diffusive fluxes are driven by concentration gradients. When Fick's first law of diffusion is applied, eq. (1) gives the standard partial differential equation of binary diffusion:

$$\frac{\partial c_S}{\partial t} = \frac{\partial}{\partial z}\left(D\,\frac{\partial c_S}{\partial z}\right) \tag{4}$$

The binary diffusion coefficient D can be a strong function of composition; however, polymer molecular weight is generally another influential parameter.[13,14] Excess free volume, if present in the solidified material, may appreciably affect the diffusion coefficient. Moreover, the presence of stress may affect the chemical potential gradients that actually drive diffusion. These possibilities are put aside here; we take D to be independent of molecular weight, excess free volume, and stress.

The boundary conditions of eq. (4) are the following. At the impermeable substrate, the flux of solvent is zero; thus,

$$D\,\frac{\partial c_S}{\partial z} = 0 \quad \text{at } z = 0,\ t > 0 \tag{5}$$

At the coating/air interface, the solvent flux relative to it on the coating side equals the solvent flux relative to it on the gas side. The latter flux is by diffusion and convection and can be represented by a mass-transfer coefficient k_g multiplied by a concentration-difference driving force; therefore,

$$\begin{aligned} n_S - c_S v_P &= -\frac{D}{1 - c_S\bar{V}_S}\,\frac{\partial c_S}{\partial z} \\ &= k_g(Hc_S - c_g^\infty) \quad \text{at} \\ z &= l(t),\ t > 0 \end{aligned} \tag{6}$$

Here c_g^∞ is the solvent concentration in the gas far from the surface and $c_S(l)$ is the solvent concentration in the liquid at the surface and in equilibrium with the solvent concentration in the gas at the surface. Parameter H is Henry's coefficient of solubility, which depends on temperature. The appropriate initial condition of uniform solvent content in a coating of given thickness is

$$c_S(z,\,0) = c_S^0, \quad 0 < z < l_0 \tag{7}$$

and the rate of change of coating thickness $l(t)$ is given by

$$\frac{dl(t)}{dt} = -\bar{V}_S k_g(Hc_S - c_g^\infty) \tag{8}$$

Strain

At the instant liquid is applied to the substrate, its solvent concentration is uniform; this we take as time zero, when diffusion begins. At that moment, each polymer-labeled material particle in

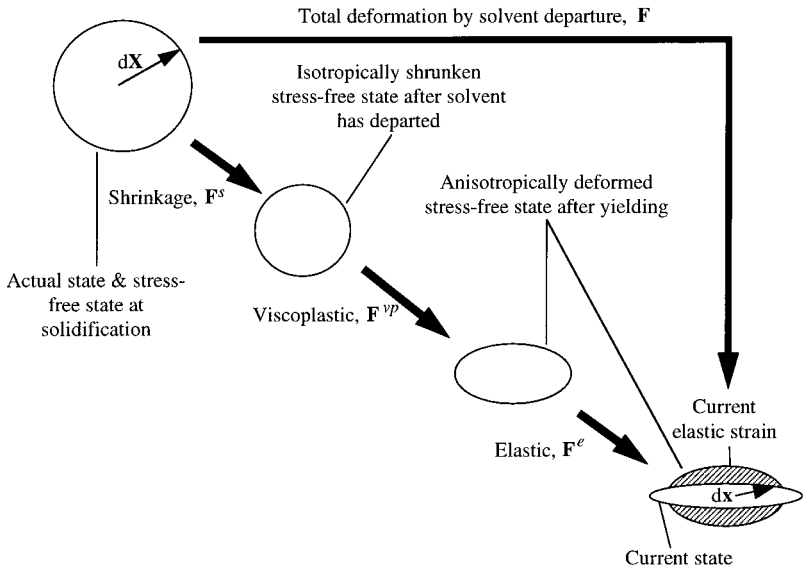

Figure 2 Local strain in a drying elasto-viscoplastic coating. The total deformation gradient **F** from position **X** in the stress-free state at solidification to position **x** in the current stressed state can be factored into three parts: volume shrinkage $\mathbf{F}^s$, viscoplastic yielding $\mathbf{F}^{vp}$, and elastic deformation $\mathbf{F}^e$.

the liquid coating is described by its distance Z_P from the substrate. As diffusion proceeds, its distance $z_P(Z_P; t)$ from the substrate diminishes. As solvent evaporates, a solidification front presumably appears at the top of the coating when the polymer concentration c_P there reaches c_P^*, the gel-transition concentration, or glass-transition concentration. Next the front propagates toward the substrate. Each particle solidifies at a certain time and a certain place where its concentration first reaches c_P^*, that is, at $t = t(Z_P; c_P^*)$ and $z_P = z_P(Z_P; c_P^*)$.

To describe how strain evolves after local solidification requires consideration of how the material deforms and how its stress-free state deforms locally as remaining solvent diffuses toward the coating surface and evaporates there. The initial stress-free reference state is taken to be the state of the polymer in the solution at the instant it solidifies, that is, when it reaches the polymer concentration c_P^* at which it first acquires elastic modulus.[3] Deformation after that is described by the change in relative locations of neighboring particles between their stress-free state at solidification and their current state. This is given by a deformation gradient with two distinct principal components: (1) the in-plane isotropic component $F_\parallel = 1$, whose magnitude is simply unity because the material moves not in xy-planes but only in the z-direction; and (2) the out-of-plane component $F_\perp$.

At any time and location within the solidified coating, the principal deformation gradient components define an oblate ellipsoid of unit major diameter (Fig. 2), the flattening of which represents the local loss of solvent. As long as the stress has not passed the yield strength, the principal components of the deformation gradient of the stress-free state follow from Amagat's law:

$$F_\parallel^s = F_\perp^s = \alpha, \quad \alpha \equiv \left(\frac{c_P^*}{c_P}\right)^{1/3} = \left(\frac{1 - c_S^* \bar{V}_S}{1 - c_S \bar{V}_S}\right)^{1/3} \tag{9}$$

in which α is the shrinkage ratio, the cubic power of which gives the ratio of current specific volume to that at solidification. Equation (9) defines a sphere of less-than-unity diameter (Fig. 2), the reduction of which is proportional to the cube root of the ratio of the concentration of polymer at solidification to its concentration, made higher by the departure of solvent through diffusion and drying. When stress has exceeded the yield strength, the stress-free state deforms viscoplastically. In that event the principal components of the total deformation gradient of the stress-free state are $\alpha F_\parallel^{vp}$ and $\alpha F_\perp^{vp}$, where $F_\parallel^{vp}$ and $F_\perp^{vp}$ are two principal components of the viscoplastic deformation gradient. The total deformation gradient of the stress-free state defines a mildly oblate spheroid (Fig. 2).

The departure of the deformation gradients of the current state from those of the (current)

stress-free state determines the (current) elastic strain, to which the (current) elastic stress is proportional. Applying the chain rule of differentiation yields

$$F^e_{\parallel} = \frac{F_{\parallel}}{F^s_{\parallel}F^{vp}_{\parallel}} = \frac{1}{\alpha F^{vp}_{\parallel}}, \quad F^e_{\perp} = \frac{F_{\perp}}{F^s_{\perp}F^{vp}_{\perp}} = \frac{F_{\perp}}{\alpha F^{vp}_{\perp}} \quad (10)$$

where the superscripts e and s denote elastic part and shrinkage part, respectively. These are rearrangements of the original form, which represents decomposition of the deformation from the initial stress-free state to the current state of stress in three successive deformation steps: (1) volume shrinkage from the initial stress-free state to an intermediate, isotropic stress-free state; (2) viscous flow and plastic deformation of this shrunken intermediate stress-free state to the current anisotropic stress-free state; and (3) elastic deformation from this current anisotropic stress-free state to the current state of stress. This is summarized in Figure 2. The second and third steps were dealt with by Lee et al.[15]; all three, by Tam et al.[9,10]:

$$F_{\parallel} = F^e_{\parallel}F^{vp}_{\parallel}F^s_{\parallel}, \quad F_{\perp} = F^e_{\perp}F^{vp}_{\perp}F^s_{\perp} \quad (11)$$

Elastic strain is properly expressed by the in-plane and out-of-plane principal components of either the left Cauchy–Green tensor $\mathbf{B}^e$ or the right Cauchy–Green tensor $\mathbf{C}^e$; in one-dimensional drying the two are the same:

$$B^e_{\parallel} = C^e_{\parallel} = (F^e_{\parallel})^2, \quad B^e_{\perp} = C^e_{\perp} = (F^e_{\perp})^2 \quad (12)$$

Any difference between the current stress-free state and the current state causes the Cauchy–Green tensors to deviate from unity; such deviation gives rise to stress, as detailed below.

In postyield viscous deformation of the stress-free state, the rate of deformation is related by so-called flow rules to the difference between current stress and yield stress. The principal components of the rate of deformation follow from the time derivative (overdot) of the deformation gradient (the in-plane component of the deformation gradient is constant, however):

$$L_{\parallel} \equiv \frac{\dot{F}_{\parallel}}{F_{\parallel}} = 0, \quad L_{\perp} \equiv \frac{\dot{F}_{\perp}}{F_{\perp}} \quad (13)$$

From eq. (11), each component can be broken into elastic, viscoplastic, and shrinkage contributions. The viscoplastic contributions of the rate of deformation gradient are

$$L^{vp}_{\parallel} = \frac{\dot{F}^{vp}_{\parallel}}{F^{vp}_{\parallel}} = \frac{\dot{F}_{\parallel}}{F_{\parallel}} - \frac{\dot{F}^e_{\parallel}}{F^e_{\parallel}} - \frac{\dot{\alpha}}{\alpha},$$

$$L^{vp}_{\perp} = \frac{\dot{F}^{vp}_{\perp}}{F^{vp}_{\perp}} = \frac{\dot{F}_{\perp}}{F_{\perp}} - \frac{\dot{F}^e_{\perp}}{F^e_{\perp}} - \frac{\dot{\alpha}}{\alpha} \quad (14)$$

Because the available yield criterion and flow rule have been formulated as applying in the current stress-free state, these material time derivatives need to be transformed to the current stress-free state.[16] In the current stress-free state they have the forms

$$\bar{L}^{vp}_{\parallel} = (F^e_{\parallel})^2 L^{vp}_{\parallel}, \quad \bar{L}^{vp}_{\perp} = (F^e_{\perp})^2 L^{vp}_{\perp} \quad (15)$$

Thus $\bar{L}^{vp}_{\parallel}$ and $\bar{L}^{vp}_{\perp}$ are the in-plane and out-of-plane viscoplastic strain rates as viewed in the current stress-free state. They are related to the stresses by the flow rule described in the next section.

Constitutive Relations

The elastic stress is modeled with the neo-Hookean equation,[17] which for one-dimensional drying gives isotropic in-plane stress and out-of-plane stress as

$$\sigma_{\parallel} = -p + \frac{G}{3}(F^{e^2}_{\parallel} - F^{e^2}_{\perp}),$$

$$\sigma_{\perp} = -p - \frac{2G}{3}(F^{e^2}_{\parallel} - F^{e^2}_{\perp}) \quad (16)$$

where p is the negative mean normal stress and must be hydrostatic pressure, because it must equal ambient pressure in the absence of deviatoric strain. G is the shear modulus, which can depend on polymer or solvent concentration (and on temperature, of course). The neo-Hookean equation is for incompressible material and is a fair approximation for polymer–solvent systems in the rubbery state, which is generally incompressible. It is used here to model polymer solutions that solidify not only by gelling but also by vitrifying. It probably approximates stress in the latter case more poorly as more solvent departs after they vitrify, because glassy polymers typi-

cally become somewhat compressible as their glass-transition temperature rises above their current temperature. The condition of incompressibility in elastic deformation is

$$F_{\parallel}^{e^2} F_{\perp}^{e} = 1 \tag{17}$$

A drying coating sustains the pressure p_a of the drying gas at its exposed surface. With the incompressibility condition, this leads to expressions for pressure and in-plane elastic stress in the coating:

$$p - p_a = -\frac{2G}{3}\left[(F_{\parallel}^{e})^2 - (F_{\parallel}^{e})^{-4}\right],$$
$$\sigma_{\parallel} = -p_a + G\left[(F_{\parallel}^{e})^2 - (F_{\parallel}^{e})^{-4}\right] \tag{18}$$

Thus, because $F_{\parallel}^{e}$ must exceed unity where a coating has in-plane tension (see Fig. 2), the pressure in such places must be subambient. This remarkable inference seems to be novel, and may have important implications (e.g., regarding solvent action in nuclei and flaws). If no plastic yielding has taken place, $F_{\parallel}^{e} = 1/\alpha$ and $F_{\perp}^{e} = F_{\perp}/\alpha = \alpha^2$ (because $F_{\perp} = c_P^*/c_P = \alpha^3$); then the pressure and in-plane stress depend only on how much solvent has departed:

$$p - p_a = -\frac{2G}{3}(\alpha^{-2} - \alpha^4) < 0,$$
$$\sigma_{\parallel} + p_a = G(\alpha^{-2} - \alpha^4) > 0 \tag{19}$$

Again, because the available yield criterion and flow rule have been formulated as applying in the current stress-free state, the Cauchy stress in the current state needs to be transformed to the current stress-free state. Doing so gives the second Piola–Kirchhoff stress tensor, whose in-plane and out-of-plane components are

$$\bar{S}_{\parallel} = -p_a \frac{F_{\perp}}{F_{\parallel}^{e^2}} + GF_{\perp}(1 - F_{\parallel}^{e^{-6}}), \quad \bar{S}_{\perp} = -p_a F_{\perp} F_{\parallel}^{e^4} \tag{20}$$

Actually, for the chosen yield criterion and flow rule, just the deviatoric part of Cauchy stress needs to be transformed to the current stress-free state:

$$\bar{S}'_{\parallel} = \frac{G}{3} F_{\perp}(1 - F_{\parallel}^{e^{-6}}), \quad \bar{S}'_{\perp} = \frac{2G}{3} F_{\perp}(1 - F_{\parallel}^{e^6}) \tag{21}$$

The second invariant of the above stress tensor is

$$\Phi = \sqrt{\frac{1}{2}(\bar{S}'_{\perp} C_{\perp}^{e})^2 + (\bar{S}'_{\parallel} C_{\parallel}^{e})^2} = \frac{G}{\sqrt{3}} \left| F_{\perp} F_{\parallel}^{e^2}(1 - F_{\parallel}^{e^{-6}}) \right| \tag{22}$$

As the drying continues and stress rises, the top surface and then deeper positions in a coating may enter an elasto-viscoplastic regime. For the present purposes of describing coating behavior after yielding, a von Mises' yield criterion and viscoplastic strain rate proportional to excess stress over yield stress (in the direction of the yield function gradient in stress space) were chosen, with no strain hardening.[16] The von Mises' yield criterion is

$$\Phi - k = \begin{cases} < 0, & \text{elastic deformation} \\ = 0, & \text{critical condition} \\ > 0, & \text{continuous yielding} \end{cases} \tag{23}$$

where k is the critical shear stress at yielding and acts to define the size of the (abstract) yield surface in the space of principal stresses (the stress having been transformed to the current stress-free state).

The flow law of yielding when the criterion is exceeded is that the rate of viscoplastic deformation is proportional to the excess of the second invariant over the yield value, and is in the direction, in the space of the principal directions, of the gradient of the second invariant:

$$\bar{L}_{\parallel}^{vp} = \frac{1}{\mu}\langle \Phi - k \rangle \frac{\partial \Phi}{\partial \bar{S}_{\parallel}} = \frac{\langle \Phi - k \rangle}{2\mu\Phi} C_{\parallel}^{e^2} \bar{S}'_{\parallel},$$
$$\bar{L}_{\perp}^{vp} = \frac{1}{\mu}\langle \Phi - k \rangle \frac{\partial \Phi}{\partial \bar{S}_{\perp}} = \frac{\langle \Phi - k \rangle}{2\mu\Phi} C_{\perp}^{e^2} \bar{S}'_{\perp} \tag{24}$$

where μ is the postyield internal viscosity of the coating, that is, the viscosity by which the stress-free state evolves toward the current state. The notation $\langle\ \rangle$ denotes

$$\langle \Phi - k \rangle = \begin{cases} \Phi - k & \text{if } \Phi > k \\ 0 & \text{otherwise} \end{cases} \tag{25}$$

With rearrangement that makes use of eqs. (12), (21), and (22), these strain rate equations simplify

Table I Dimensionless Variables and Parameters Used

Solvent concentration $c \equiv c_S/c_S^0$	Equilibrium concentration $c_{eq} \equiv c_g^\infty/(Hc_S^0)$
Time $\tau \equiv D_0 t/l_0^2$	Initial volume fraction $\beta_i \equiv \bar{V}_S c_S^0$
Location $\eta \equiv z/l(t)$	Sherwood number $\mathrm{Sh} \equiv k_g l_0 H/D_0$
Particle position $\eta_p \equiv z_p/l(t)$	Solidification volume fraction $\beta_c \equiv \bar{V}_S c_S^*$
Surface position $\lambda \equiv l(t)/l_0$	Elasticity number $N_{El} \equiv G_0 l_0^2/(\mu_0 D_0)$
Stress $\sigma \equiv (\sigma_\| + p_a)/G_0$	Yield stress $\kappa = k_0/G_0$
Diffusion function $f = D(c)/D_0$	Modulus function $g = G(c)/G_0$
Viscosity function $m = \mu(c)/\mu_0$	Yield stress function $n = k(c)/k_0$

to two differential equations that govern the development of the current stress-free state:

$$\frac{\dot{F}_\|^{vp}}{F_\|^{vp}} = \frac{G}{6\mu}\left(\alpha F_\perp^{vp} - \alpha^7 F_\perp^{vp} F_\|^{vp^6} - \sqrt{3}\,\frac{k}{G}\,\frac{1-\alpha^6 F_\|^{vp^6}}{|1-\alpha^6 F_\|^{vp^6}|}\right) \tag{26}$$

$$\frac{\dot{F}_\perp^{vp}}{F_\perp^{vp}} = -\frac{G}{3\mu}\left(\alpha F_\perp^{vp} - \alpha^7 F_\perp^{vp} F_\|^{vp^6} - \sqrt{3}\,\frac{k}{G}\,\frac{1-\alpha^6 F_\|^{vp^6}}{|1-\alpha^6 F_\|^{vp^6}|}\right) \tag{27}$$

These two equations differ only by a constant. Eliminating the common term on the right and applying the initial condition of $F_\|^{vp} = F_\perp^{vp} = 1$ reveal that the viscoplastic deformation is indeed incompressible:

$$F_\|^{vp^2} F_\perp^{vp} = 1 \tag{28}$$

Hence, one of the two differential equations about development of the stress-free state becomes unnecessary. Eliminating $F_\perp^{vp}$ between eqs. (26) and (27) leaves the single ordinary differential equation

$$\frac{\dot{F}_\|^{vp}}{F_\|^{vp}} = \frac{G\alpha^3}{6\mu}\left(\frac{1}{\alpha^2 F_\|^{vp^2}} - \alpha^4 F_\|^{vp^4} - \sqrt{3}\,\frac{k}{G\alpha^3}\,\frac{1-\alpha^6 F_\|^{vp^6}}{|1-\alpha^6 F_\|^{vp^6}|}\right) \tag{29}$$

This one equation, replicated at a sufficient number of levels in a coating, together with the diffusion equation system (4)–(8) are enough to describe one-dimensional drying and stress development.

Summary of Equations in Dimensionless Form

In polymer–solvent systems, the diffusion coefficient is a strong function of concentration,

$$D = D_0 f(c_S) \tag{30}$$

where $f(c_S)$ is a monotonically rising function of solvent concentration. Mechanical properties, which appear after solidification, also depend on solvent concentration. Shear modulus, yield stress, and postyield viscosity can be expressed as products of terminal values and monotonically falling functions of solvent concentration:

$$G = G_0 g(c_S), \quad \mu = \mu_0 m(c_S), \quad k = k_0 n(c_S) \tag{31}$$

In this way the variable properties are measured in units that make them of the order of unity or less.

With the dimensionless variables and parameters defined in Table I, eqs. (4)–(8) and (29) can be put in convenient dimensionless form. In Table I, the Sherwood number Sh is the ratio of internal resistance to mass transfer in the coating to external mass transfer resistance in the air or gas outside it. The elasticity number N_{El} is the ratio of a characteristic diffusion time to a characteristic time of viscoplastic deformation of the stress-free state. The resulting dimensionless equation system is

$$\frac{\partial c}{\partial \tau} = \frac{1}{\lambda^2}\frac{\partial}{\partial \eta}\left(\frac{D(c)}{D_0}\frac{\partial c}{\partial \eta}\right) + \frac{\eta}{\lambda}\frac{d\lambda}{d\tau}\frac{\partial c}{\partial \eta} \tag{32}$$

$$\frac{d\lambda}{d\tau} = -\beta_i \mathrm{Sh}(c - c_{eq}) \tag{33}$$

$$c(\eta, 0) = 1, \quad \lambda(0) = 1$$

$$c_\eta(0, \tau) = 0, \quad \frac{f}{1-\beta_i c}\, c_\eta(1, \tau) = -\mathrm{Sh}\lambda(c - c_{eq}) \tag{34}$$

$$F_\|^{vp} = 1 \quad \text{before yielding } (\Phi < k) \tag{35}$$

$$\frac{1}{F_{\parallel}^{vp}}\frac{dF_{\parallel}^{vp}}{d\tau}=\frac{gN_{El}\alpha^3}{6m}$$
$$\times\left(\frac{1}{\alpha^2F_{\parallel}^{vp^2}}-\alpha^4F_{\parallel}^{vp^4}-\sqrt{3}\,\frac{\kappa n}{g\alpha^3}\,\frac{1-\alpha^6F_{\parallel}^{vp^6}}{|1-\alpha^6F_{\parallel}^{vp^6}|}\right)$$
upon yielding (36)

$$\alpha=\left(\frac{1-\beta_c}{1-\beta_i c}\right)^{1/3} \tag{37}$$

Because the in-plane viscoplastic deformation of the stress-free state does not affect diffusion here (although it might in reality, through the diffusivity), diffusion eqs. (32)–(34) can be solved independently of the ordinary differential eq. (36). Hence the entire course of drying can be found first, and then the development of stress at each level in the coating follows from eqs. (10), (16)–(19), and (35)–(37).

Galerkin/Finite-Element Solution

The quantitative predictions of solvent concentration in the next section were made by solving eqs. (32)–(34) by the Galerkin's weighted residual method with finite-element basis functions. The approximation solution to the concentration field is

$$c\approx\sum_{i=1}^{N}c_i(\tau)\phi^i \tag{38}$$

where ϕ^i are the total number of N quadratic, one-dimensional basis functions and $c_i(\tau)$ their unknown coefficients. The Galerkin form of eq. (32) is given by

$$\int_0^1\left[\frac{\partial c}{\partial\tau}-\frac{1}{\lambda^2}\frac{\partial}{\partial\eta}\left(\frac{D(c)}{D_0}\frac{\partial c}{\partial\eta}\right)-\frac{\eta}{\lambda}\frac{d\lambda}{d\tau}\frac{\partial c}{\partial\eta}\right]$$
$$\phi^j\,d\eta=0,\quad j=1,2,\ldots,N \tag{39}$$

Integrating the second-derivative term by parts and using the boundary conditions in eq. (34) give

$$\int_0^1\frac{\partial c}{\partial\tau}\phi^j\,d\eta+\frac{1}{\lambda^2}\int_0^1\frac{D(c)}{D_0}\frac{\partial c}{\partial\eta}\frac{\partial\phi^j}{\partial\eta}\,d\eta-\frac{1}{\lambda}\frac{d\lambda}{d\tau}\int_0^1$$
$$\eta\frac{\partial c}{\partial\eta}\phi^j\,d\eta+\frac{\mathrm{Sh}}{\lambda}(1-\beta_i c)(c-c_{eq})\phi^j|_{\eta=1}=0,$$
$$j=1,\ldots,N \tag{40}$$

When the concentration is substituted by the approximation eq. (38), we have N ordinary differential equations. When combined with eq. (33), they can be solved for unknowns c_i ($i=1,\ldots,N$) and λ. In the present study, the time derivatives in eqs. (33) and (40) are approximated by the first-order, implicit Euler integration with fixed time steps.

For all the results in the next section, the computation domain $0\le\eta\le1$ was spanned by 20 quadratic elements. They diminished quadratically in size toward the surface (the length of each was the square root of that of its more distant neighbor), to resolve the steep concentration gradient at the start of the drying. Small enough time steps were chosen such that a further decrease did not alter the predictions by more than 0.5%. At each time step, Newton iteration was used to solve the nonlinear equations for the values of the coefficients of the basis functions; the iteration began with their values from the previous step. Within each iteration the linear algebraic equation system was solved by Gauss elimination with partial pivoting. The iteration was terminated when the norms of both the residuals and the concentration updates at all nodes were less than 10^{-8}; choosing a tighter tolerance affected the predictions by less than 0.1%.

At each time step the particle positions $z_P(Z_P, t)$ were found by integrating the concentration of polymer between the particle and the substrate; the integral remains constant:

$$\int_0^{z_P}c_P(z_P,t)\,dz=c_P^0Z_P \tag{41}$$

At each time step the shrinkage ratio α was found versus concentration from eq. (9). The position was found where the polymer concentration reached c_P^*, the solidification value. There were three successive regimes in time: (1) c_P^* had not yet been reached at $\eta=1$, that is, $c_P<c_P^*$ throughout, and none of the coating was solidified; (2) c_P^* lay in the internal $0\le\eta\le1$, that is, the solidification front was in the coating; and (3) c_P^* had been reached at $\eta=0$, that is, $c_P>c_P^*$ throughout, and all of the coating was solidified.

In similar fashion the position of the yield front was found. At positions where the coating was solid, that is, $c_P>c_P^*$, stress and pressure versus shrinkage ratio were found from eq. (19) and the quantity Φ was evaluated from eq. (22). As deep

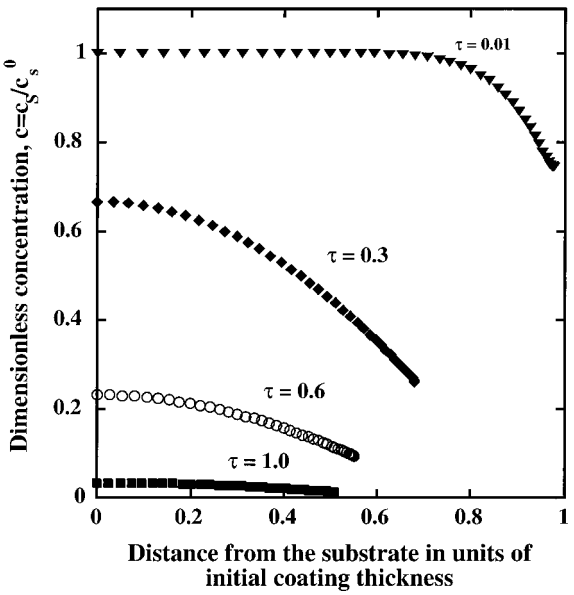

Figure 3 Concentration distribution through the coating thickness at four dimensionless times: $\tau = 0.01$, $\tau = 0.3$, $\tau = 0.6$, and $\tau = 1$. The parameters used are Sherwood number Sh = 5, equilibrium concentration $c_{eq} = 0$, initial volume fraction $\beta_i = 0.5$, solidification volume fraction $\beta_c = 0.1$, elasticity number $N_{El} = 4$, and yield stress parameter $\kappa = 0.05$. The Sh chosen is that of the internal resistance controls. This need not always be the case, and there can be a very small concentration gradient when Sh is much less than 1.

into the coating as Φ exceeded k, yielding had begun and eq. (36) was solved for $F_{\|}^{vp}$, from which elastic stress $\sigma_{\|}$ was found from eqs. (10) and (18). With continued drying, shrinkage and in-plane stress both rise. Once the stress exceeds the yield value, it tends to relax back to that value but it cannot reach lower values unless the coating is reswelled with solvent or compressed in-plane by force applied externally.

For the predictions in the next section, Henry's law coefficient H and the mass transfer coefficient k_g were taken to be independent of concentration, as were the quantities f, g, m, and n in eqs. (30) and (31). At each time step, the in-plane stress $\sigma_{\|}$ was calculated versus position z_P; it was then integrated over and divided by the coating thickness to arrive at predictions of average stress.

RESULTS

Figure 3 shows the concentration profile taken at four different times: $\tau = 0.01$, $\tau = 0.3$, $\tau = 0.6$, $\tau = 1.0$. The parameters used are Sh = 5, $c_{eq} = 0$, $\beta_i = 0.5$, $\beta_c = 0.1$, $N_{El} = 4.0$, $\kappa = 0.05$. At the start of drying, a large driving force causes rapid solvent depletion near the surface, resulting in a steep concentration profile, as shown at $\tau = 0.01$. In the late stages of drying, the solvent in the coating is almost in equilibrium with solvent vapor in the air and the concentration profile is flat throughout the coating.

As drying proceeds and the concentration profile develops, the polymer is most concentrated at the coating/air surface. Once it reaches c_P^*, it solidifies at the coating/air interface first, then this solidification front propagates into the coating until it finally reaches the substrate. Further solvent depletion and shrinkage after solidification induces in-plane stress, and when the local stress is high enough (above the yield stress) the coating yields locally. Therefore, there also exists a yield front, which in this case also starts at the coating/air interface and propagates into the coating toward the substrate. There is a delay from the solidification front to the yield front. Coating ahead of the solidification front is still in the liquid state, in which only hydrostatic pressure is considered. Coating particles between the solidification front and yield front are within the elastic region, in which the stress and pressure can be directly evaluated from eq. (19). Coating particles behind the yield front are subject to elasto-visco-plastic deformation, in which the evaluation of stress requires solving ordinary differential eq. (36). The propagation of the solidification front and the yield front is shown in Figure 4, where the positions of the fronts are normalized by the current thickness, to identify the start of solidification and yielding. The parameters used are the same as those in Figure 3.

By varying β_i the model predicts how stress evolves in coatings with different initial solvent concentrations (see Fig. 5). Stress evolves faster in initially more concentrated coatings because the coating glass-transition temperature (which increases as solvent leaves) reaches the actual experimental temperature earlier than do coatings with larger initial solvent amounts. This effect was shown experimentally by Croll and others.[3,18] The numerical solution suggests that final stress is independent of the initial solution concentration. For an elastic coating, this is a straightforward conclusion because the in-plane stress is related to the shrinkage ratio after solidification by eq. (19), and the final shrinkage ratio, according to eq. (9), is related to the solvent concentration only at the solidification point and at

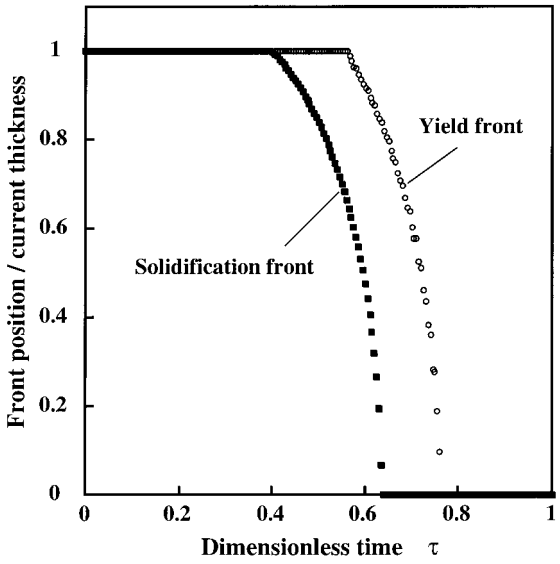

Figure 4 The propagation of solidification front and yield front. The yield front is behind the solidification front. Parameters Sh = 5, c_{eq} = 0, β_i = 0.5, β_c = 0.1, N_{El} = 4, κ = 0.05. Concentration dependence of material properties is ignored.

the end of drying. Hence, the model also predicts that final stress magnitudes are independent of final coating thickness because the coatings of different initial concentrations cast at the same thickness will dry to various thicknesses.

EXPERIMENTAL

From the preceding results the model predicts that final stress magnitudes are independent of initial solution concentration and final coating thickness, a finding that agrees with the experimental data of Croll, Perera, and others.[3–5,18] Thus, the model qualitatively predicts what is observed in practice. However, for the model to be most useful, it must be able to predict how stress evolves, not just the final coating stress. This ability will allow investigators to understand how and when stress develops and then to tailor a manufacturing process accordingly. To improve our understanding, the model results are compared to actual stress evolution data taken using a cantilever-deflection technique.[19] A schematic of the device is shown in Figure 6.

Materials Preparation

Polyisobutyl methacrylate, PIBM (Elvacite 2045, ICI Acrylics Inc., Cordova, TN), polystyrene, PS (18242-7; Aldrich Chemical Co., Milwaukee, WI), or polyvinyl butyral, PVB (B76; Monsanto Chemical Co., Japan) were dissolved in toluene to give initial coating concentrations of 10 to 30 wt % polymer. The solutions were then delivered by syringe onto substrates clamped on one end. These were steel feeler gauge stock of thickness 0.15 to 0.45 mm, cut to 6 mm in width and clamped to give a cantilever length of 45 mm. At this width-to-length ratio the cantilever was calculated to cup negligibly as it bent (i.e., the strain was essentially planar). By means of a motor drive, the substrate was drawn at about 0.7 cm/s beneath a fixed coating blade with a preset coating gap. Gaps of 100 to 400 μm were used, which yielded wet layers about 50 to 200 μm thick. Once the substrate was coated, the coating was dried by a stream of nitrogen at 21°C flowing at approximately 0.8 cm/s (50 cm^3/min through a 10-cm^2 cross section).

Solutions of 8 wt % gelatin in deionized water at pH 5.4 and 45°C were prepared by stirring and were coated in the same way, except that the coating apparatus was preheated throughout to 45°C, and the coated layer plus its substrate were chilled at 5°C before drying began. The gelatin was a sensitizing grade supplied by Eastman Kodak Company (Rochester, NY; Lot 30-060). Following certain industrial practice, chill times of 30–60 s were used for coatings 50 to 200 μm

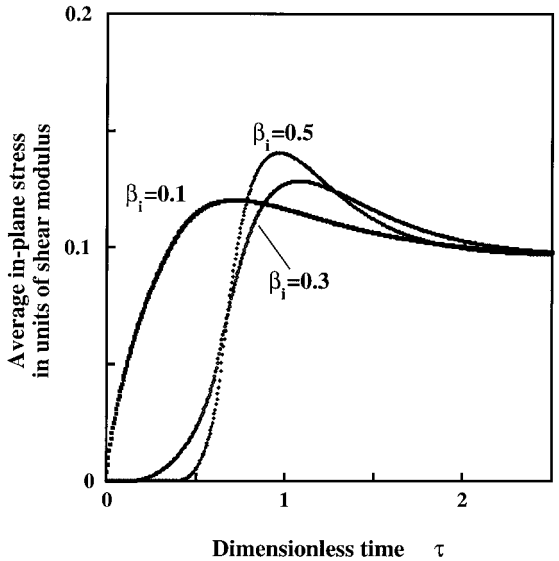

Figure 5 The development of average in-plane stress in drying. This shows the effect of initial solvent concentration. Parameters used are Sh = 5, c_{eq} = 0, β_c = 0.1, κ = 0.05, N_{El} = 4.

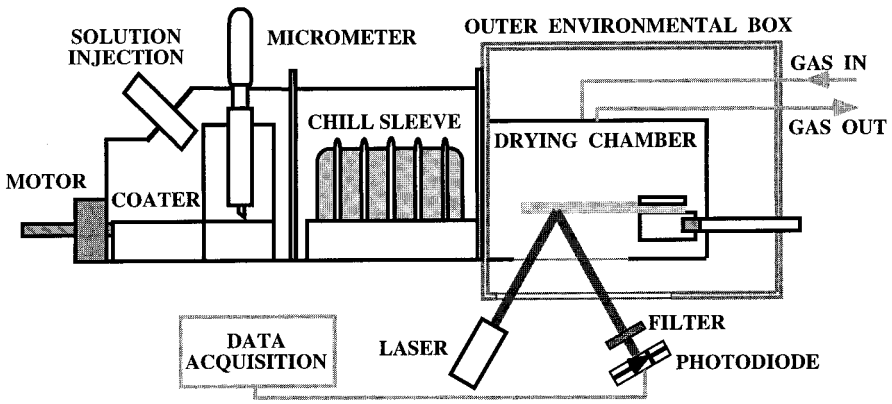

Figure 6 Schematic of the stress-measurement apparatus consisting of controlled environment combination draw-down coater, chill box, and cantilever stress-measurement system.

thick; the purpose was to gel the gelatin solutions by cooling them to 28 to 35°C, depending on gelatin content. The coatings were then dried in nitrogen streams of temperature and relative humidity ranging from 20°C and 0% RH to 58°C and 69% RH.

Stress Measurement Apparatus

The controlled-environment microbatch coating, drying, and stress-measurement apparatus is shown in Figure 6 and described in detail elsewhere.[18,19] Stress was measured on the principle of bending deflection of a bilayer cantilever when the upper layer is in uniform in-plane isotropic tensile stress that is negligibly relieved by the deflection, and the lower layer, by virtue of its thickness, modulus, and Poisson ratio, has more than 10^5-fold greater flexural rigidity than that of the upper layer. In these circumstances the in-plane tensile stress can be evaluated with a modified version of Corcoran's[20] formula:

$$\sigma = \left[\frac{EH_S^3}{12(1-\nu^2)}\right]\frac{4d(1+\nu)}{hL^2(H_S+h)} \qquad (42)$$

Here the term in brackets is the flexural rigidity of the substrate; H_S and L are its thickness and length, respectively; E, which bending beam experiments showed to be 170 GPa, is the substrate modulus; and ν is its Poisson ratio, 0.29; d is the deflection of its free end; and h is the coating thickness. For the experimental results shown here, the final coating thickness is used to calculate stress. This is an acceptable assumption, based on the conclusion that most stress will evolve after the coating has reached a solid state, that is, a majority of the solvent has evaporated.

DISCUSSION

The first step in modeling stress evolution is understanding the mechanical/rheological behavior of the coating. By varying κ, the ratio of the yield stress k_0 to the shear modulus G_0, we can get varying gradations of coating mechanical behavior. Figure 7 shows the elastic ($\kappa = \infty$), elasto-viscoplastic ($\kappa = 0.05$), and the viscoelastic ($\kappa = 0$) limit of the elasto-viscoplastic behaviors of a drying coating. In the purely elastic coating, the in-plane average stresses increase monotonically to a plateau magnitude. An example of this is shown in Figure 8, where stress was measured for PS, PVB, and PIBM coatings cast in toluene. These polymers are glassy in their pure form at the experimental temperature and thus behave in a mostly elastic fashion. Explanations for the different stress levels measured for the various polymers can be found elsewhere.[18] Elasto-viscoplastic behavior can be shown by the curve with $\kappa = 0.05$ (Fig. 7), in which stress rises because of drying and postsolidification volume shrinkage, reaches a maximum, and then relaxes to a constant. Gelatin coatings cast in water and dried at relative humidity above 0% (at 20°C) provide a good example of elasto-viscoplastic behavior (see Fig. 9). At $\kappa = 0$ (Fig. 7), the coating behaves more like a viscous material rather than a solid. The viscous stress rises, relaxes, and diminishes to zero. This type of behavior might be expected in fast-drying systems where the polymer glass-

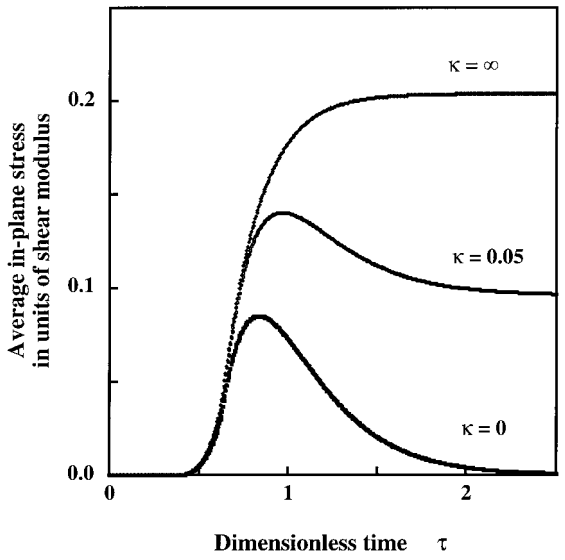

Figure 7 The development of average in-plane stress in drying. By varying the parameter κ, stress development can be modeled in coatings cast from elastic, viscoelastic, or elasto-viscoplastic materials. The parameters used are Sh = 5, $c_{eq} = 0$, $\beta_i = 0.5$, $\beta_c = 0.1$, $N_{El} = 4$. Concentration dependence of material properties is ignored.

transition temperature is significantly lower than the drying temperature. In practice, the behavior observed is most likely a combination of the aforementioned situations. Coatings tend to start as a

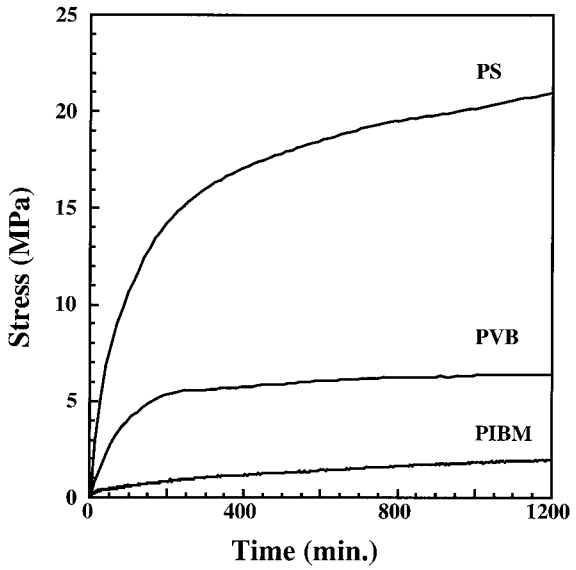

Figure 8 Experimental stress evolution in polystyrene (PS), polyvinyl butyral (PVB), and polyisobutyl methacrylate (PIBM) coatings cast in toluene and dried under nitrogen.

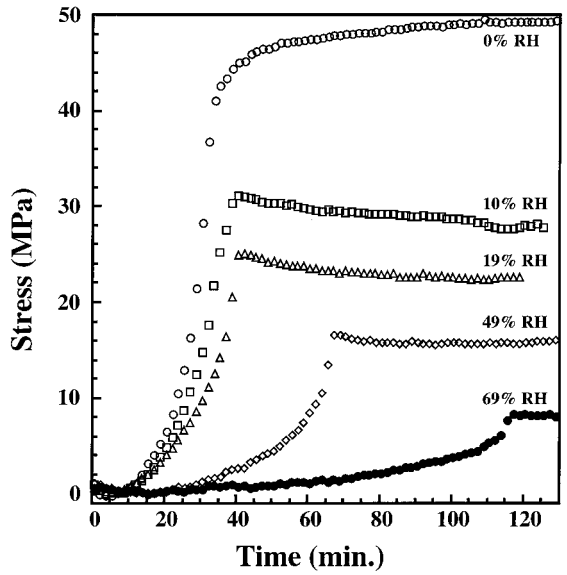

Figure 9 Stress evolution in gelatin coatings dried at 20°C and different levels of relative humidity.

viscous fluid, then transform (as solvent leaves the coating) to elasto-viscoplastic, and finally, in some cases, reach a more glassy, elastic state; thus, the rate at which solvent is removed plays a crucial role in determining how much stress remains in a dried coating.

One way to control the rate of drying is by varying the solvent vapor concentration in air. The effect of solvent vapor concentration in air can be shown by varying c_{eq}, the equilibrium solvent volume fraction (Fig. 10). More vapor in the air slows drying, and therefore slows the rate at which stress evolves. The final stress level decreases at higher equilibrium solvent fraction because of less overall postsolidification shrinkage. Gelatin–water systems demonstrate this type of behavior (see Fig. 9). Figure 10 also shows when solvent concentration in the vapor is so high (e.g., at equilibrium solvent fractions 0.06 and 0.09), the stress is not great enough to go above the yield stress and the coating behaves elastically.

This drying rate dependence suggests processing history plays a key role in understanding stress evolution. Our model can help elucidate what can occur by varying different processing conditions. For instance, cycling the relative humidity (by varying c_{eq}) of drying air can lower the maximum stress level. This is shown in Figure 11, where coatings are initially dried at different c_{sw} for a certain period of time (where Sh = 4, $\beta_i = 0.3$, $\beta_c = 0.1$, $\kappa = 0.02$, $N_{El} = 0.05$, and $\Delta\tau = 0.05$). After the solvent in the coating reaches

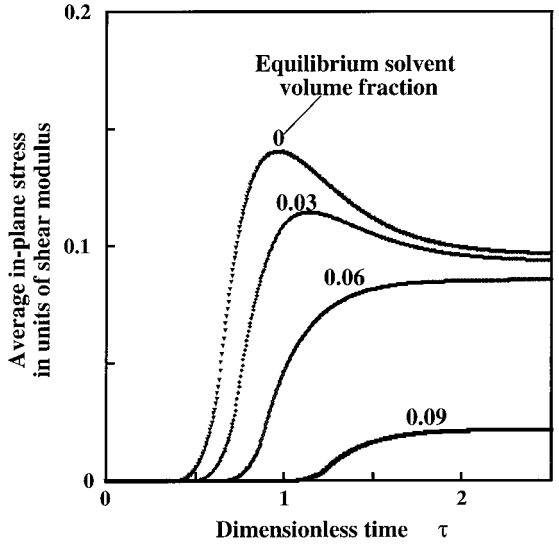

Figure 10 The development of average in-plane stress in drying. Stress development in coatings drying at different levels of humidity can be modeled by varying the parameter c_{eq}. The parameters used are Sh = 5, $\beta_i = 0.5$, $\beta_c = 0.1$, $\kappa = 0.05$, $N_{El} = 4$.

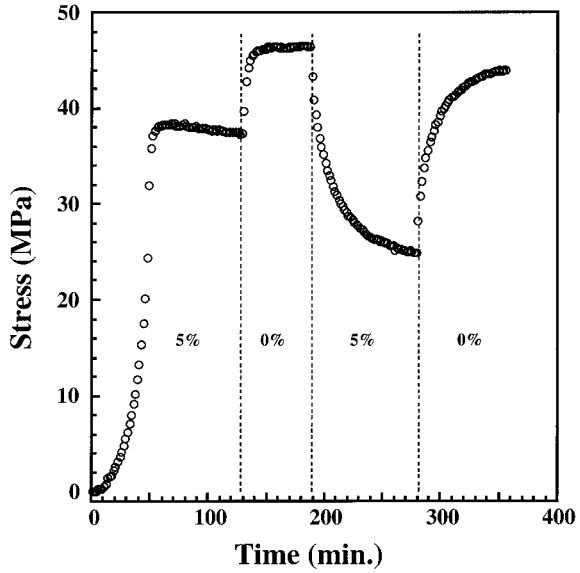

Figure 12 Stress relaxation after initial stress development for a gelatin coating dried at 20°C and 5% RH. Relative humidity was cycled between 5 and 0%.

equilibrium with that present in the air, the relative humidity c_{eq} is reduced to 0% from $3 < \tau \leq 5$. This leads to further solvent loss and higher stresses. The drying air is then cycled back to c_{sw}, causing the coatings to swell and the stresses to fall accordingly. However, because of irreversible plastic deformation that was generated during plastic yielding and a change in the stress-free state, the stress levels after cycling are lower than those before cycling. Such history dependence is evident when gelatin–water systems are exposed to relative-humidity cycling.[18,21] An experimental example of this is shown in Figure 12 for a gelatin coating initially dried at 5% RH and 20°C.

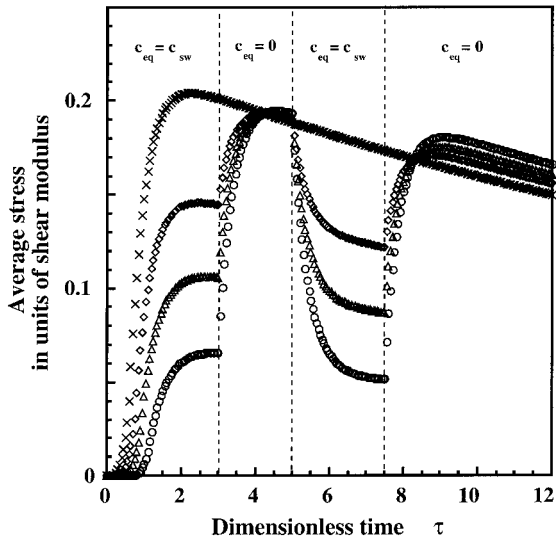

Figure 11 The effect of cycling relative humidity on development of average in-plane stress. The parameters used are Sh = 4, $\beta_i = 0.3$, $\beta_c = 0.1$, $\kappa = 0.02$, $N_{El} = 0.05$, and $\Delta\tau = 0.05$. c_{sw} is the dimensionless solvent concentration in air. (○, $c_{sw} = 0.07$; △, $c_{sw} = 0.05$; ◇, $c_{sw} = 0.03$, ×, $c_{sw} = 0$).

As mentioned in the previous section, N_{El} is the ratio of characteristic diffusion time to characteristic viscous relaxation time. A large N_{El} corresponds to a small viscous relaxation time, leading to fast stress relaxation, whereas a smaller N_{El} gives slower stress relaxation. This is shown in Figure 13. Moreover, a smaller N_{El} corresponds to a higher maximum stress level. At $N_{El} = 0.1$, the stress relaxes slowly and the coating behaves very nearly like an elastic material. Another extreme limit is shown at $N_{El} = 100$, which corresponds to a very short relaxation time. In this case, the relaxation time is so short that, whenever the stresses go above the yield surface, they relax back to the yield surface almost instantaneously, behaving like a perfectly plastic material.

To make more quantitative comparisons, one needs to determine the concentration-dependent materials properties (modulus, yield stress, etc.). Some of the necessary data exist in the literature, although a much more intensive experimental

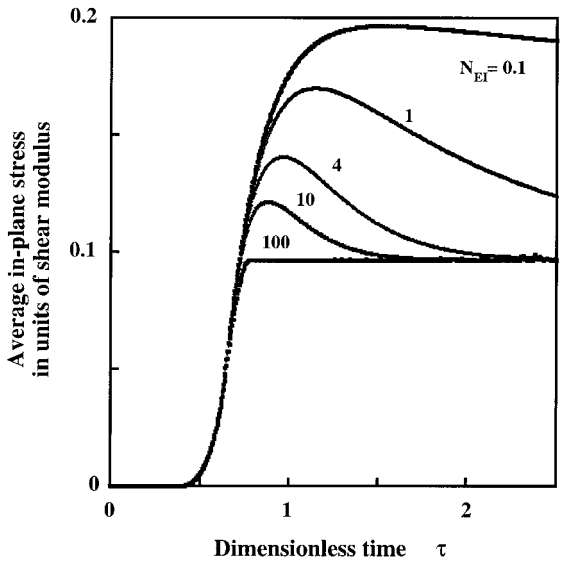

Figure 13 The development of average in-plane stress in drying. Stress development in coatings cast from materials with different characteristic diffusion times and different viscoplastic deformations of stress-free state is modeled by varying the parameter N_{El}. The parameters used are Sh = 5, $\beta_i = 0.1$, $\kappa = 0.01$, $c_{eq} = 0.6$.

study for specific coating systems would be required to make the predictions accurate.

CONCLUSIONS

A large deformation elasto-viscoplastic model was developed to predict stress development in drying coatings. When coupled with mass transport equations, the static equilibrium equation was solved by the Galerkin/finite-element method in the one-dimensional coating. Computation was compared with experimental measurements of stresses in solvent-cast homopolymer and aqueous gelatin coatings.

The model suggests that final stress in the coating is independent of final coating thickness and initial liquid concentration. This prediction agrees well with experimental stress measurements in polymer coatings cast in toluene and in aqueous gelatin coatings.

The solvent vapor content in the air not only decreases the final stress but also slows the stress development; this is because vapor in the air will lower the driving force for drying. This effect was clearly shown by modeling and by experiments on gelatin coatings dried at different levels of relative humidity. Calculations on the effect of relaxation time suggest that, at slow relaxation times, stresses can reach far above the yield surface and then slowly relax; however, with fast relaxation times, the stresses quickly relax whenever the stresses go above the yield surface.

This research was supported by the Center for Interfacial Engineering, an NSF-sponsored Engineering Research Center at the University of Minnesota, through its Coating Process Fundamentals Program; and by the DuPont Company, through a Young Professor's Grant to L.F.F. The authors are grateful to K. S. A. Chen, S.-Y. Tam, and S. Weinstein for helpful discussions; and to P. R. Petersen, J. T. Kern, and W. T. Gruhlke for their technical assistance.

REFERENCES

1. Cohen, E. D.; Gutoff, E. B. Modern Coating and Drying Technology; VCH Publishers: New York, 1992.
2. Sato, K. Prog Org Coat 1980, 8, 143.
3. Croll, S. G. J Appl Polym Sci 1979, 23, 847.
4. Perera, D. Y.; Eynde, D. V. J Coat Technol 1981, 53, 39.
5. Perera, D. Y.; Eynde, D. V. J Coat Technol 1983, 55, 37.
6. Hasatani, M.; Itaya, Y. Drying Technol 1992, 10, 1013.
7. Hasatani, M.; Itaya, Y.; Muroie, K. Drying Technol 1993, 11, 815.
8. Itaya, Y.; Mabuchi, S.; Hasatani, M. Drying Technol 1995, 13, 801.
9. Tam, S. Y.; Scriven, L. E.; Stolarski, H. K. Mater Res Soc Symp Proc 1995, 356, 547.
10. Tam, S. Y. Ph.D. Thesis, University of Minnesota, 1997.
11. Christodoulou, K. N.; Lightfoot, E. J.; Powell, R. W. Am Inst Chem Eng J 1998, 44, 1484.
12. Bird, R. B.; Steward, W. E.; Lightfoot, E. N. Transport Phenomena; Wiley: New York, 1960.
13. Vrentas, J. S.; Vrentas, C. M. Macromolecules 1994, 27, 4684.
14. Cairncross, R. A.; Francis, L. F.; Scriven, L. E. Drying Technol 1992, 10, 893.
15. Lee, E. H. J Appl Mech 1969, 91, 1.
16. Moran, B.; Ortiz, M.; Shih, C. F. Int J Numer Methods Eng 1990, 29, 483.
17. Rivlin, R. S.; Saunders, D. W. Philos Trans R Soc London Ser A 1951, 243, 251.
18. Payne, J. A. Ph.D. Thesis, University of Minnesota, 1998.
19. Payne, J. A.; McCormick, A. V.; Francis, L. F. Rev Sci Instrum 1997, 68, 4564.
20. Corcoran, E. A. J Paint Technol 1969, 41, 635.
21. Payne, J. A.; McCormick, A. V.; Francis, L. F. J Appl Polym Sci 1999, 73, 553.